2000

On the bosonic spectrum of QCD (1+1) with SU(N) currents

Uwe Trittmann
Otterbein University

ELSEVIER

Nuclear Physics B 587 (2000) 311–327

NUCLEAR PHYSICS B

www.elsevier.nl/locate/npe

On the bosonic spectrum of QCD(1 + 1) with $SU(N)$ currents

Uwe Trittmann

Department of Physics, Ohio State University, Columbus, OH 43210, USA

Received 22 May 2000; revised 14 July 2000; accepted 19 July 2000

Abstract

In this note we calculate the spectrum of two-dimensional QCD. We formulate the theory with $SU(N_c)$ currents rather than with fermionic operators. We construct the Hamiltonian matrix in DLCQ formulation as a function of the harmonic resolution K and the numbers of flavors N_f and colors N_c. The resulting numerical eigenvalue spectrum is free from trivial multi-particle states which obscured previous results. The well-known 't Hooft and large N_f spectra are reproduced. In the case of adjoint fermions we present some new results.

PACS: 11.15.-q; 11.10.Ef; 11.40.-q; 11.10.St
Keywords: $SU(N)$ gauge field theory; Current algebra; Bosonization; Mass spectrum; Light front quantization; Dimension 2

1. Introduction

On the way to understand the physics of strong interactions, two-dimensional QCD has remained an interesting model ever since it has been studied by 't Hooft [1]. It has, however, the disadvantage of lacking dynamical (i.e., transverse) gluonic degrees of freedom. To construct a model closer to four-dimensional QCD, adjoint rather than fundamental fermions were built into the theory [2,3]. Also matter with a large number of flavors has been considered [4,5]. Surprisingly, these theories are related by a universality [6]: the massive spectrum and interactions of two-dimensional Yang–Mills theories coupled to massless fermions in arbitrary representations depend only on the gauge group and the level of the affine Lie algebra. The associated parameter space of two-dimensional Yang–Mills theories with massless fermions is depicted in Fig. 1 [7].

Of particular interest in two-dimensional QCD is the transition between confinement and screening. The 't Hooft model is known to consist of stable mesons and has no

E-mail address: trittman@pacific.mps.ohio-state.edu (U. Trittmann).

0550-3213/00/$ – see front matter
PII: S0550-3213(00)00469-7

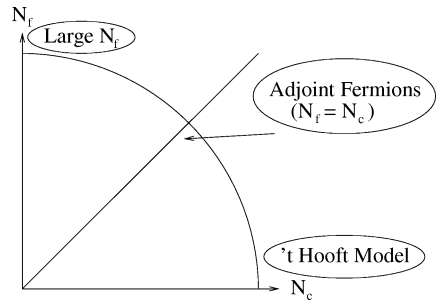

Fig. 1. The parameter space of two-dimensional Yang–Mills theories with massless fermions.

confinement-screening transition. The model with adjoint fermions exhibits deconfinement at zero fermion mass m, and the string tension vanishes like $\sigma \propto m$ at this point [8–11]. Interestingly, this theory is supersymmetric at the fermion mass $m^2 = g^2 N_c$, and asymptotically supersymmetric otherwise. It has been studied extensively in the literature [2,3,12–14]. We will focus on the massless case of this theory, where we can make use of the universality [6], and consequently we will formulate the theory as a current algebra problem. The Hilbert space of the problem then splits up into current sectors. This allows for a convenient reduction of the numerical effort when solving for the spectrum of the theory, since all single-particle states lie in the current block of the identity (bosons) or in the adjoint current block (fermions) [6]. Because of its simpler algebraic properties, we will limit ourselves in the present work to the bosonic spectrum. We will use the additional parameter in the problem, $\lambda = N_f/N_c$, as a tool for interpreting the spectrum, i.e., we will consider theories 'on the arc' of Fig. 1, where both N_c and N_f are large. The main emphasis will be on the adjoint case (N_c=N_f). The goal is to identify the single-particle states of the theories and to be able to connect to results anticipated from the asymptotic theory, e.g., the expected multi-Regge trajectory structure in the adjoint case [3].

A very convenient way to formulate two-dimensional QCD is to quantize the system on the light-cone [1]. Usually the light-cone gauge, $A^+ = 0$, is used. This approach gives a very complete picture and includes non-perturbative effects, if an appropriate regularization for the quark self-energy is used [15]. Discretized Light Cone Quantization (DLCQ) [16,17] is then a method especially suited to solve numerically for the spectrum of low dimensional theories. The momenta are discretized by imposing boundary conditions on the fields. The typical DLCQ program is to construct a finite-dimensional Hamiltonian matrix characterized by the harmonic resolution K. The spectrum is obtained by diagonalizing this matrix numerically for larger and larger K, and eventually extrapolating to the continuum limit, $K \to \infty$.

The latest large N_c analysis of adjoint QCD_2 [12] revealed several single-particle states and, most interestingly, a continuum of states at precisely four times the mass (squared) of the lowest fermion state. Despite this remarkable structure, the insight gained from this finding is rather small. It is clearly not a signature for screening versus confinement. Both in a confining and a screening theory, one would expect a continuum of states at $4m^2$ of a single-particle state, although from very different mechanisms. More information about

the spectrum is thus needed to understand things like the deconfinement mechanism or the statistics of single-particle states.

The paper is organized as follows. In the following section we review two-dimensional QCD with massless fermions. Section 3 deals with analytic considerations. Namely, we show that it is possible to calculate two eigenvalues of the theory from the outset. In Section 4.1 we construct the Hamiltonian matrix for any harmonic resolution K and arbitrary (i.e., in principle finite) N_f and N_c. We will, however, *in praxi* only use the large N limit of this result. Section 4 details the numerical results. We will focus on the adjoint case, but also consider the 't Hooft limit and the large N_f limit to present a coherent picture of two-dimensional QCD. A discussion of the results follows.

2. QCD in two dimensions

We want to compute the massive spectrum of $SU(N_c)$ Yang–Mills gauge fields coupled to massless adjoint fermions in two dimensions. Due to the universality in these gauge theories [6], this is equivalent to solving for the massive spectrum of $N_f = N_c$ flavors of massless fundamental Dirac fermions coupled to the gauge fields. The latter case turns out to be more general, in the sense that we have an additional continuous parameter, $\lambda := N_f/N_c$, in the theory. The case of adjoint gauged fermions is recovered when setting λ to unity. Without loss of generality we consider only the Lagrangian of the fundamental theory

$$\mathcal{L} = \mathrm{Tr}\left[-\frac{1}{4g^2} F_{\mu\nu} F^{\mu\nu} + i \sum_{a=1}^{N_f} \overline{\Psi}_a \gamma_\mu D^\mu \Psi_a \right], \tag{1}$$

where $\Psi_a = 2^{-1/4} \binom{\psi_a}{\chi_a}$, with ψ_a and χ_a carrying color indices, which we suppressed. The field strength is $F_{\mu\nu} = \partial_\mu A_\nu - \partial_\nu A_\mu + i[A_\mu, A_\nu]$, and the covariant derivative is defined as $D_\mu = \partial_\mu + i A_\mu$. We work in the light-cone gauge $A^+ = 0$ and use the convenient Dirac basis $\gamma^0 = \sigma_1$, $\gamma^1 = -i\sigma_2$. The Lagrangian then becomes

$$\mathcal{L} = \mathrm{Tr}\left[\frac{1}{2g^2} (\partial_- A_+)^2 + i\psi^\dagger \partial_+ \psi + i\chi^\dagger \partial_- \chi - A_+ J \right], \tag{2}$$

with the current $J_{ij} = \psi^\dagger_{ia} \psi_{aj}$. We can integrate out the (non-dynamical) component A_+ of the gauge field and obtain

$$\mathcal{L} = \mathrm{Tr}\left[i\psi^\dagger \partial_+ \psi + i\chi^\dagger \partial_- \chi - \frac{g^2}{2} J \frac{1}{\partial_-^2} J \right]. \tag{3}$$

It is obvious that the left-movers χ decouple. Noting the simple expression of the interaction in terms of the currents, it is natural to bosonize the theory [18]. We follow Ref. [5] to derive the momentum operators. The bosonized action of colored flavored fermions is

$$S_0 = S^{\mathrm{WZW}}_{(N_f)}(g) + S^{\mathrm{WZW}}_{(N_c)}(h) + \frac{1}{2} \int d^2x \, \partial_\mu \phi \, \partial^\mu \phi, \tag{4}$$

where $g \in SU(N_c)$, $h \in SU(N_f)$, $\exp\{i\sqrt{\frac{4\pi}{N_c N_f}}\phi\} \in U_B(1)$, and the Wess–Zumino–Witten action is

$$S^{\mathrm{WZW}}_{(k)}(g) = \frac{k}{8\pi}\int_{\Sigma} d^2x\ \mathrm{Tr}\big(\partial_\mu g \partial^\mu g^{-1}\big) + \frac{k}{12\pi}\int_{B} d^3y\,\epsilon^{ijk}\,\mathrm{Tr}\big(g^{-1}\partial_i g\big)\big(g^{-1}\partial_j g\big)\big(g^{-1}\partial_k g\big), \tag{5}$$

where B is the solid sphere whose boundary Σ represents space–time. The action of the theory is then

$$S = S_0 + \frac{g^2}{2}\int d^2x\, J\frac{1}{\partial_-^2}J, \tag{6}$$

with the currents $J = \frac{ik}{2\pi} g\partial_- g^{-1}$ generating a level N_f affine $SU(N_c)$ Kac–Moody algebra. The associated energy-stress tensor $T^{\mu\nu}$ yields the momentum operators

$$P^+ = T^{++} = \frac{\pi}{N_c + N_f}\int_{-\infty}^{\infty} dx^- : J_{ij}(x^-)J_{ji}(x^-) : , \tag{7}$$

$$P^- = T^{+-} = -\frac{g^2}{2}\int_{-\infty}^{\infty} dx^- : J_{ij}(x^-)\frac{1}{\partial_-^2}J_{ji}(x^-) : . \tag{8}$$

To obtain the mass eigenvalues M_n we have to solve the eigenvalue problem

$$2P^+P^-|\psi\rangle = M_n^2|\psi\rangle, \tag{9}$$

which is equivalent to diagonalizing the operator P^-, since P^+ is already diagonal. To discretize the system, we impose periodic boundary conditions of length $2L$ on the currents, $J_{ij}(-L) = J_{ij}(+L)$, and expand them into a discrete series of modes

$$J_{ij}(x^-) = \frac{1}{\sqrt{2}L}\sum_{n=-K}^{K} J_{ij}(n)e^{-ix^-(2\pi n)/L}, \tag{10}$$

with

$$J_{ij}(n)|0\rangle = 0 \quad \forall n > 0. \tag{11}$$

The cutoff $K \equiv P^+L/(2\pi)$ controls the coarseness of the momentum-space discretization. The continuum limit is obtained by sending K to infinity. The modes of the currents obey the algebra

$$\big[J_{ij}(n), J_{i'j'}(n')\big] = nN_f\left(\delta_{ij'}\delta_{i'j} - \frac{1}{N_c}\delta_{ij}\delta_{i'j'}\right)\delta^n_{-n'} + \delta_{ij'}J_{i'j}(n+n') - \delta_{i'j}J_{ij'}(n+n'). \tag{12}$$

The momentum generators

$$P^+ = \left(\frac{2\pi}{L}\right)\frac{1}{N_c+N_f}\sum_{n=1}^{K} J_{ij}(-n)J_{ji}(n), \tag{13}$$

$$P^- = \frac{\widetilde{g}^2}{2\pi}\sum_{n=1}^{K}\frac{1}{n^2}J_{ij}(-n)J_{ji}(n), \tag{14}$$

are finite-dimensional matrices on the Hilbert space constructed by acting with the current operators on the vacuum defined in Eq. (11). For convenience we introduced the scaled coupling $\widetilde{g}^2 = g^2L/(2\pi)$. Note that the box length L drops out of the eigenvalue problem, Eq. (9). At large N_c we expect the Fock basis to consist of single-trace states

$$\frac{1}{N_c^s}\operatorname{Tr}\big[J(-n_1)J(-n_2)\cdots J(-n_s)\big]|0\rangle.$$

We note that a cyclic permutation of the currents will reproduce these states only up to states with a lower number of currents. The number of currents is not conserved.

3. Analytic considerations

The discretization of momenta via the DLCQ procedure puts severe constraints on the possible Fock states. It turns out that they allow for the *a priori* calculation of two of the eigenvalues. At harmonic resolution K the states

$$|K\rangle = \operatorname{Tr}\big[\{J(-1)\}^K\big]|0\rangle, \tag{15}$$

$$|K-1\rangle = \operatorname{Tr}\big[\{J(-1)\}^{K-2}J(-2)\big]|0\rangle \tag{16}$$

are unique and have K and $K-1$ currents, respectively. The sectors with less than $K-1$ currents contain more than one state, e.g.,

$$|K-2\rangle_1 = \operatorname{Tr}\big[\{J(-1)\}^{K-3}J(-3)\big]|0\rangle, \tag{17}$$

$$|K-2\rangle_s = \operatorname{Tr}\big[\{J(-1)\}^{K-2-s}J(-2)\{J(-1)\}^{s-2}J(-2)\big]|0\rangle, \quad 2\leqslant s\leqslant\frac{K}{2}. \tag{18}$$

It is relatively straightforward to derive the expressions

$$P^-|K\rangle = \frac{\widetilde{g}^2}{2\pi}(N_c+N_f)K|K\rangle + \mathcal{O}\big(|K-1\rangle\big), \tag{19}$$

$$P^-|K-1\rangle = \frac{\widetilde{g}^2}{2\pi}(N_c+N_f)\left(K-\frac{3}{2}\right)|K-1\rangle + \mathcal{O}\big(|K-2\rangle\big), \tag{20}$$

$$P^-|K-2\rangle_i = 0 + \mathcal{O}\big(|K-2\rangle\big), \tag{21}$$

where $\mathcal{O}(|p\rangle)$ are terms involving states with p or less currents. Let the dimension of the discrete Fock space be d and define $\mu_1 := (\widetilde{g}^2/(2\pi))(N_c+N_f)K$ and $\mu_2 := (\widetilde{g}^2/(2\pi))(N_c+N_f)(K-3/2)$. Then the structure of the Hamiltonian matrix is

$$P^- = \left(\begin{array}{c|cc} A & 0 & \\ \hline B & \begin{matrix}\mu_2 & 0\\ C & \mu_1\end{matrix} & \end{array}\right). \tag{22}$$

The matrices A and B have dimensions $(d-2)\times(d-2)$ and $2\times(d-2)$, respectively and C is a real number. Clearly, μ_1 and μ_2 are two eigenvalues of P^-. The eigenvalues of the mass squared operator are then

$$M_1^2 = \frac{g^2 N_c}{\pi}(1+\lambda)K^2 \quad \text{and} \quad M_2^2 = \frac{g^2 N_c}{\pi}(1+\lambda)K\left(K-\frac{3}{2}\right). \tag{23}$$

These eigenvalues seem to diverge in the continuum limit, which would render them physically irrelevant. However, one can show that the eigenvalues $M_i^2(K)$ lie in different Z_2 sectors for even and odd K and therefore cannot be connected. They rather mark the appearance of new states in the spectrum, as we will see.

4. Numerical calculations

4.1. The Hamiltonian

In this section we address to calculate the eigenvalues of QCD_2 by solving the eigenvalue problem, Eq. (9), numerically. Since the operator P^+ is already diagonal, we have to construct the action of the Hamiltonian P^- on a basis state.[1] Using the large N_c limit implies that the basis states be of the form $\mathrm{Tr}[J_1\cdots J_b]|0\rangle$, i.e., single-trace states. The current operators are subject to the Kac–Moody algebra, Eq. (12). Annihilation operators may thus be produced by *commuting* operators. The main obstacle for the calculations is to find a scheme to organize the terms in a convenient way. We obtain such a scheme by separating terms containing annihilation operators from those that do not. In the definition

$$[A,B] := \lceil A,B\rceil + \lfloor A,B\rfloor, \tag{24}$$

$\lceil A,B\rceil$ denotes the part of a commutator which consists solely of creation operators. Its complement $\lfloor A,B\rfloor$ contains annihilation operators. It is possible to write down an expression for P^- which involves only commutators of the first type and creation operators. It reads

$$P^- J_1 J_2\cdots J_b|0\rangle = \sum_{p=1}^{n}\sum_{k_1<k_2<\cdots<k_p}^{b} J_1\cdots J_{k_1-1}J_{k_1+1}\cdots J_{k_2-1}J_{k_2+1}\cdots J_{k_p-1} \times \lceil\lfloor\cdots\lfloor P^-, J_{k_1}\rfloor, J_{k_2}\rfloor,\ldots, J_{k_p}\rceil J_{k_p+1}\cdots J_b|0\rangle. \tag{25}$$

The commutators in this expression, and thus the Hamiltonian matrix, are linear in N_f by construction. To construct the Hamiltonian matrix, we have to evaluate all 2^b-1 commutators. In the worst case scenario we would have an exponentially growing number of terms $((3/2)\sum_{p=1}^{p} 2^{2(p-1)}p!b!/(b-p)!)$ in the Hamiltonian, due to the $(3/2)2^{2(p-1)}$ terms in a commutator involving p currents. Fortunately, the number of terms of leading power in N_c grows only quadratically, like $(2b-1)b$. We developed a computer code to evaluate Eq. (25) symbolically. This task exceeds typical workstation capabilities at

[1] A continuum version of the first step of this DLCQ calculation can be found in Ref. [5].

$b \geqslant 7$. It is however possible to deduce the expression for arbitrary b, because a repeated pattern evolves. In the large N_c limit the action of P^- on a state $|\mathbf{b}; n_1, \ldots, n_b\rangle := \frac{1}{N_c^b} J^{j_1}_{j_2}(n_1) \cdots J^{j_b}_{j_1}(n_b)|0\rangle$ with b currents is then

$$
\begin{aligned}
&P^-|\mathbf{b}; n_1, \ldots, n_b\rangle \\
&\quad = -\frac{\widetilde{g}^2 N_c}{2\pi} \sum_{i=1}^{b} \left(\sum_{m=1}^{n_i-1} \frac{1}{(m-n_i)^2} - \sum_{m=1}^{n_i-1} \frac{1}{m^2} \right) |\mathbf{b}+\mathbf{1}; n_1, n_2, \ldots, n_i - m, m, \ldots, n_b\rangle \\
&\qquad + \frac{\widetilde{g}^2 N_c}{2\pi} \sum_{i=1}^{b} \left(\frac{\lambda}{n_i} + \sum_{m=1}^{n_i-1} \frac{1}{m^2} \right) |\mathbf{b}; n_1, n_2, \ldots, n_b\rangle \\
&\qquad + \frac{\widetilde{g}^2 N_c}{2\pi} \sum_{i=1}^{b-1} \left(\sum_{m=0}^{n_{i+1}-1} \frac{1}{(m+n_i)^2} - \sum_{m=1}^{n_{i+1}-1} \frac{1}{m^2} \right) \\
&\qquad \times |\mathbf{b}; n_1, n_2, \ldots, n_i + m, n_{i+1} - m, \ldots, n_b\rangle \\
&\qquad + \frac{\widetilde{g}^2 N_c}{2\pi} \left(\sum_{m=0}^{n_b-1} \frac{1}{(m+n_1)^2} - \sum_{m=1}^{n_b-1} \frac{1}{m^2} \right) |\mathbf{b}; n_2, \ldots, n_{b-1}, n_b - m, n_1 + m\rangle \\
&\qquad + \lambda \frac{\widetilde{g}^2 N_c}{2\pi} \sum_{j=1}^{b-2} \Bigg\{ (-)^j \sum_{i=1}^{b-j} \left[\frac{1}{(\sum_{q=i}^{j+i} n_q)^2} - \frac{1}{(\sum_{q=i+1}^{j+i} n_q)^2} \right] n_{i+j} \\
&\qquad\qquad \times \left| \mathbf{b}-\mathbf{j}; n_1, \ldots, n_{i-1}, \sum_{q=i}^{j+i} n_q, n_{j+i+1}, \ldots, n_b \right\rangle \\
&\qquad\qquad + (-)^{j-1} \left[\frac{1}{(n_1 + \sum_{q=b-j+1}^{b} n_q)^2} - \frac{1}{(\sum_{q=b-j+1}^{b} n_q)^2} \right] n_b \\
&\qquad\qquad \times \left| \mathbf{b}-\mathbf{j}; n_2, \ldots, n_{b-j}, n_1 + \sum_{q=b-j+1}^{b} n_q \right\rangle \\
&\qquad\qquad + (-)^j \sum_{i=1}^{j-1} \left[\frac{1}{(n_1 + \sum_{q=b-i+1}^{b} n_q)^2} - \frac{1}{(\sum_{q=b-i+1}^{b} n_q)^2} \right] n_b \\
&\qquad\qquad \times \left[\left| \mathbf{b}-\mathbf{j}; n_{j-i+1}, n_{j-i+2}, \ldots, n_{b-i-1}, \sum_{q=1}^{j-i} n_q + \sum_{q=b-i}^{b} n_q \right\rangle \right. \\
&\qquad\qquad\quad \left. - \left| \mathbf{b}-\mathbf{j}; n_{j-i+2}, n_{j-i+3}, \ldots, n_{b-i}, \sum_{q=1}^{j-i+1} n_q + \sum_{q=b-i+1}^{b} n_q \right\rangle \right] \Bigg\} \\
&\qquad + \frac{\widetilde{g}^2 N_c}{2\pi} \sum_{j=1}^{b-2} \Bigg\{ (-)^j \sum_{i=1}^{b-j-1} \sum_{m=0}^{n_{i+j+1}-1} \left(\frac{1}{(m + \sum_{q=i}^{i+j} n_q)^2} - \frac{1}{(m + \sum_{q=i+1}^{i+j} n_q)^2} \right) \\
&\qquad\qquad \times \left| \mathbf{b}-\mathbf{j}; n_1, n_2, \ldots, \sum_{q=i}^{i+j} n_q + m, n_{i+j+1} - m, n_{i+j+2}, \ldots, n_b \right\rangle
\end{aligned}
$$

$$
\begin{aligned}
&+(-)^j\left(\sum_{m=0}^{n_b-1}\frac{1}{(m+n_1)^2}-\sum_{m=1}^{n_b-1}\frac{1}{m^2}\right)\\
&\times\left|\mathbf{b}-\mathbf{j};n_{j+2},\ldots,n_{b-1},n_b-m,\sum_{q=1}^{j+1}n_q+m\right\rangle\\
&+(-)^{j-1}\left(\sum_{m=0}^{n_b-1}\frac{1}{(m+n_1)^2}-\sum_{m=1}^{n_b-1}\frac{1}{m^2}\right)\\
&\times\left|\mathbf{b}-\mathbf{j};n_{j+1},\ldots,n_{b-1},\sum_{q=1}^{j}n_q+n_b\right\rangle\Bigg\}. \qquad (26)
\end{aligned}
$$

Note that only the terms in lines two and six of this result contain N_f. These terms will be absent in the 't Hooft limit ($N_f/N_c \to 0$) and will be dominant in the large N_f limit.

4.2. Numerical results

We are solving the eigenvalue problem, Eq. (9), numerically to obtain the mass spectrum. Recall that we have two parameters at our disposal to study the spectra. One is the harmonic resolution K, which we are supposed to send to infinity. The other is the ratio of the numbers of flavors and colors, $\lambda = N_f/N_c$, of the fermions in the theory. The most prominent cases are $\lambda = 0, 1, \infty$, namely, the 't Hooft limit, adjoint fermions, and the large N_f limit. Note that also the unphysical parameter K might give insight into the spectrum, e.g., the discovery of continuum states via their characteristic K dependence in Ref. [12].

The advantages of formulating the problem with $SU(N)$ currents rather than with fermionic degrees of freedom are twofold. For one, the much smaller basis allows for a larger resolution K and thus for more accurate results. We will also see the structure of the spectrum much clearer, in the sense that many, if not all, of the uninteresting multi-particle states are absent. Secondly, we are able to study the behavior of the spectrum as we couple the gauge field to different forms of matter by varying the parameter N_f/N_c, which is an algebraic variable in the present approach. This might be used a tool to interpret spectra.

Performing the numerical calculation, we obtain exactly the same eigenvalues in the adjoint case as in previous works [14] with *anti-periodic* boundary conditions for the fermions. The number of states grows exponentially with the harmonic resolution, cf. Table 1. At $K = 12$ we are diagonalizing a Hamiltonian of dimensions[2] 350×350, whereas in the fermionic approach one would have to operate on a Fock space with 4338 states to obtain the same accuracy. To further reduce the computational effort, we can use the Z_2 symmetry of the Hamiltonian which is invariant under the transformation

[2] It is not clear *a priori* how to construct a Fock basis for the current operators. A naive expectation is that single-trace states modulo cyclic permutations provide such a basis. We convinced ourselves that this is actually the correct choice by explicitly performing a large N_c Gram–Schmidt orthonormalization for small K on these states.

Table 1
Number of basis states as a function of the harmonic resolution K

K	2	3	4	5	6	7	8	9	10	11	12	13	14
States	1	2	4	6	12	18	34	58	106	186	350	630	1180

$\mathcal{T} J_{ij}(n) = -J_{ij}(n)$. It is straightforward to convince one-self that the action of this operator on a state with b currents is

$$\mathcal{T}|\mathbf{b}; n_1, n_2, \ldots, n_b\rangle = (-)^b \sum_{i=0}^{2^{b-2}} \big|\mathbf{p_i}; n_1, T_i(n_b, n_{b-1}, \ldots, n_2)\big\rangle, \tag{27}$$

where the T_i consist of p_i partial sums of the $b-1$ momenta, in the sense that i runs over all possibilities to place $0, 1, \ldots, b-2$ commas between the momenta while summing those momenta which are not separated by a comma, e.g.,

$$\begin{aligned}\mathcal{T}|\mathbf{4}; n_1, n_2, n_3, n_4\rangle = {} & |\mathbf{4}; n_1, n_4, n_3, n_2\rangle + |\mathbf{3}; n_1, n_4 + n_3, n_2\rangle \\ & + |\mathbf{3}; n_1, n_4, n_3 + n_2\rangle + |\mathbf{2}; n_1, n_4 + n_3 + n_2\rangle.\end{aligned} \tag{28}$$

In order not to complicate the construction of the Hamiltonian, we determine the Z_2 parity of an eigenstate *a posteriori* by calculating the expectation value of the operator $\mathcal{T}$ in this state. The separation of the Z_2 odd and even eigenfunctions is useful when interpreting the results, because it reduces the density of eigenvalues to roughly a half.

4.3. The 't Hooft limit

To test the consistency of our approach, we compare to the well-known results in the large N_c and the large N_f limit. We find complete agreement. First let us consider the large N_c (or 't Hooft) limit, where we should recover the results of the 't Hooft model [1]. The spectrum of large N_c QCD in two dimensions with massless fundamental fermions asymptotically has the form $M^2 = \pi^2 n$ for large integer n, where the mass squared is in units $g^2 N_c/\pi$. We find that at $K = 14$ the lowest ten single-particle states have masses [3]

$$M^2 = 5.88, 14.11, 23.04, 32.27, 41.68, 51.24, 60.93, 70.76, 80.97, 90.90, \tag{29}$$

which is in very good agreement with 't Hooft's numerical solution [1]. The actual spectrum, Fig. 2, is a mixture of single- and multi-particle states. The multi-particle states decouple completely from the single-particle states. They appear here, because we do not use an orthonormal basis. We have performed a calculation with an orthonormal set of states up to $K = 6$ and found that then only single-particle states are present. We were able to identify all multi-particle states as composites of two or more single-particle states. The masses M^2_{mp} of multi-particle states is given by [12]

[3] We performed the continuum limit here and in the sequel by fitting the data to a polynomial of second degree in $1/K$.

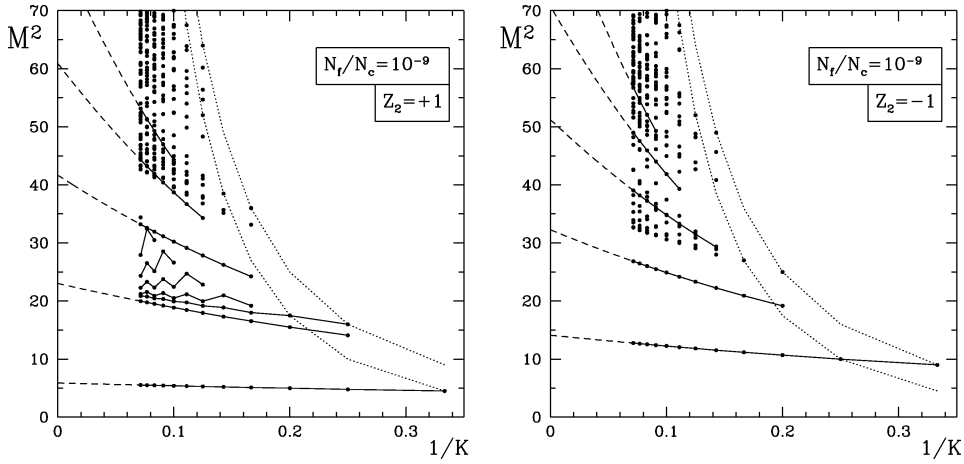

(a) (b)

Fig. 2. Spectra of the 't Hooft limit in the Z_2 even (a) and odd (b) sectors. Solid lines connect associated eigenvalues as K varies. Short dashed lines connect analytically calculable eigenvalues. Long dashed lines are extrapolations towards the continuum limit. Masses are in units $g^2 N_c/\pi$.

$$\frac{M^2_{\rm mp}(K)}{K} = \frac{M^2_{p_1}(n)}{n} + \frac{M^2_{p_2}(K-n)}{K-n}, \tag{30}$$

where $M^2_{p_i}(n)$ are the masses of single-particle states at harmonic resolution n. These masses are exactly reproduced in the spectrum. This identification in turn made it possible to detect the single-particle states hidden amongst the multi-particle states. Surprisingly, the eigenfunctions have no significant structure, apart from the special form of the lowest state in each Z_2 sector. In particular, we were unable to distinguish single- from multi-particle wavefunctions by their shapes.

4.4. Adjoint fermions

Consider now the adjoint spectrum, Fig. 3. If we look at the eigenvalue trajectories (mass squared as a function of K), the structure of the spectrum looks similar to the 't Hooft case. We see immediately three single-particle candidates which qualify by their straight, smooth trajectories. In the continuum limit they have the eigenvalues

$$M^2_{B_1} = 10.84, \qquad M^2_{B_2} = 25.73, \qquad M^2_{B_3} = 45.66. \tag{31}$$

The expectation for the asymptotic solution is here [3]

$$M^2_{n_1,n_2,\ldots,n_k} = 2\pi^2(n_1 + n_2 + \cdots + n_k), \quad n \in 2\mathbf{Z}, \tag{32}$$

again in units $g^2 N_c/\pi$. The single-particle masses appear to be at roughly twice the values of the 't Hooft limit, whereas the low-lying 'multi-particle'[4] masses stay at more or

[4] We use quotation marks here and in the following because it is not *a priori* clear that these states are indeed multi-particle states.

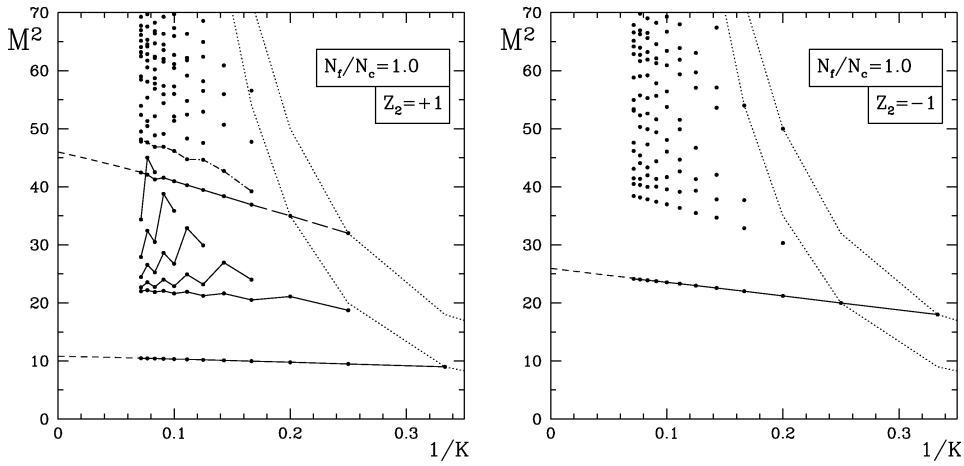

(a) (b)

Fig. 3. Spectra of the theory with adjoint fermions in the Z_2 even (a) and odd (b) sectors. Solid lines connect associated eigenvalues as K varies. Short dashed lines connect analytically calculable eigenvalues. Dashed lines are extrapolations towards the continuum limit. Masses are in units g^2N_c/π. The dash-dotted trajectory is the analog of the third single-particle state in the 't Hooft limit.

less their 't Hooft values. The crucial difference between the spectra is that the 'multi-particle' eigenvalues of the adjoint case coincide only approximately with the values from the mass formula, Eq. (30). They are systematically lower than expected. As such, these states appear to be loosely *bound* composites, i.e., they have to be interpreted as single-particle states, at least at finite K. We can see that these states are a vital part of the spectrum by comparing the eigenvalues at $M^2 \simeq 32$, $K = 13$ in Fig. 2(a) with those of Fig. 3(a) at $M^2 \simeq 42$, $K = 12$. In the latter case the eigenvalues repel each other, leading to a deformation of the eigenvalue trajectory of the (conjectured) single-particle state B_3. This means that the 'multi-particle' states are interacting! By varying the parameter λ, we were able to follow this deformation. As N_f grows, the lowest multi-particle states of the 't Hooft spectrum 'move through' the single-particle state with mass squared $M^2 = 23.04$ in the 't Hooft limit, and produce these deformations in a trajectory. In the 't Hooft limit, Fig. 2(a), we see no distortion of the single-particle trajectory though the corresponding eigenvalue is almost degenerate with a (decoupled) multi-particle state. [5]

The question arises, whether these loosely bound states become multi-particle states and decouple in the continuum limit in the adjoint spectrum. For the states between $M^2 = 20$ and $M^2 = 40$ in the Z_2 even sector, the answer is certainly yes. We performed a fit to the data finding that the eigenvalues converge towards a single point, namely the two particle continuum threshold at $M^2 = 22.85 = 4M_{F_1}^2$, i.e., twice the mass of the lowest fermionic

[5] The same deformation occurs in the fermionic spectrum, namely in the trajectory of the second Z_2 even single-particle state of Ref. [12].

state [12]. The deviations from the mass formula, Eq. (30), vanishes faster than $1/K^{\beta}$, where $\beta > 2$.

The deformation of a trajectory renders it questionable if the associated state is really a single-particle state. As K grows there will be more and more 'multi-particle' states to distort the trajectory. On the other hand, the 'multi-particle' sector will interact less and less as K increases. The number of (low-lying) 'multi-particle' states grows linearly with K. If we can take the deviation of the 'multi-particle' states from the mass formula (proportional to $1/K^{\beta}$) as a measure of the coupling, we have to conclude that the single-particle trajectory will be less and less distorted and thus a true single-particle state will emerge as $K \to \infty$. Although the first two points of the trajectory at $K = 4$ and $K = 5$ are multi-particle states with fermionic constituents, [6] we feel quite safe about the single particle nature of this state, because we find that the same situation occurs in the case of the lowest Z_2 odd trajectory, which represents undoubtedly a single-particle state, due to its complete isolation in the spectrum. To check whether all 't Hooft mesons become adjoint single-particle states, we followed the next two Z_2 even single-particle trajectories of the 't Hooft spectrum as we varied λ in small steps. One is shown as the dashed-dotted line in Fig. 3 just above the state converging to $M^2 = 45.99$. Their irregular shape makes it unlikely that they are single-particle states.

The eigenfunctions and the probability distributions in parton number were helpful to identify states at different K in the fermionic formulation of the theory [2,12]. Here, with a non-conserved parton number, these quantities will be of limited usefulness. In the fermionic formulation the single-particle states have a high probability to be states of a definite parton number [2]. In the present work, we find this behavior only for the lowest state in the Z_2 even sector, cf. Fig. 4(a). This state is a two current state to a very good approximation (98.4%). The next-to-lowest state is an almost perfect mixture of two and three parton states, although this ratio varies with K. We definitely cannot use information about the probability distributions to distinguish states: if we have a close encounter of two eigenvalues in the spectrum, one of which is presumably a single- and the other one a multi-particle state, we find that the probability distributions are almost identical. For the higher states significant structures in the parton probability distributions are missing altogether. Concerning the wavefunctions, we find that the lowest eigenstate is a single peak in the two-particle sector, cf. Fig. 4(a). We find no obvious structure in other states that could give a hint of how to construct solutions of the theory analytically. However, there might be hints of an additional structure in the eigenfunctions: we found several wavefunctions which have a noticeable amplitude drop at the boundaries of parton number sectors. As an example, consider the drop of the wavefunctions of the 'single-particle' states (B_1, B_2, B_3) at the boundaries of the $2, 3$, and 4 current sectors, respectively in Fig. 4(b). The 'multi-particle' state $(M^2 = 22.03)$ does not exhibit such a behavior. In principle, the wavefunction should factorize if it is a continuum state consisting of two non-interacting bound states. Disentangling wavefunctions along these lines has been attempted

[6] One state consists of $M^2_{F_1}(K = 5/2) = 5$ and $M^2_{F_2}(K = 5/2) = 12.5$, the other of the first mass plus $M^2_{F_2}(K = 3/2) = 9$.

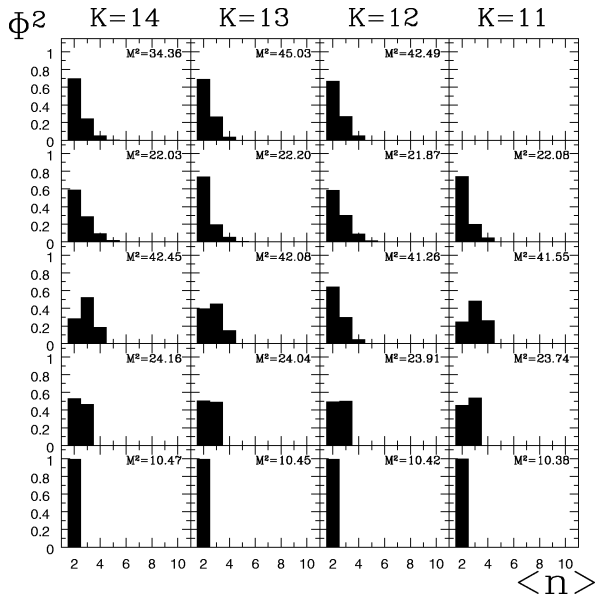

(a)

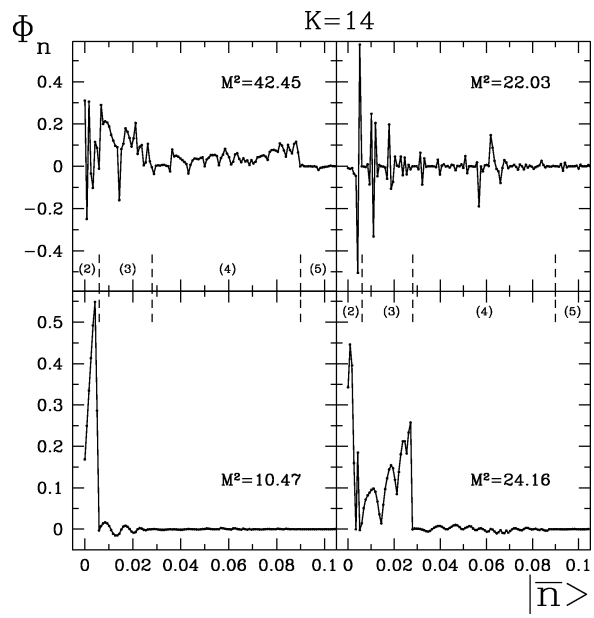

(b)

Fig. 4. Adjoint fermions: (a) The current number distribution functions of selected states at different harmonic resolution K. The lower three rows are distributions of (conjectured) single-particle states. The state in the top row is not present at $K = 11$. (b) Wavefunctions of selected eigenstates at $K = 14$ as functions of the basis state number divided by the total number of states (1180). The dashed lines mark points of changing parton content (number of currents in parenthesis).

in Ref. [23]; here, however, this task seems intractable, due to the non-conserved parton number.

4.5. Large N_f limit and intermediate cases

When going over to the large N_f limit, $\lambda \to \infty$, the operator P^-, Eq. (26), has a dominant kinetic term. In the two-particle truncation the spectrum is purely kinematical. In the full theory a residual interaction is present. In the spectrum, Fig. 5(a), we see a continuum of states starting at $M^2 = 4g^2 N_f/\pi$. The only particle in the spectrum is thus a meson with mass $M_M^2 = g^2 N_f/\pi$. This is in full agreement with results from analytic calculations [7]. The Z_2 odd sector looks similar, with the continuum starting at $M^2 = 9 = 3^2 M_M^2$. The single-particle state is absent in our calculations due to the tracelessness of the currents, i.e., the absence of the one current state.

Let us look at the eigenvalues as a function of N_f/N_c. Fig. 5(b) shows the first[7] calculation of the spectrum of two-dimensional Yang–Mills theories as a function of the continuous parameter N_f/N_c. We see that the (low-lying) trajectories are linear, as is expected from the analytic calculations in Section 3. The parameter N_f actually plays a role similar to that of a mass term in the 't Hooft model [20]. Indeed, the curves obtained by taking the continuum limit of the single-particle trajectories in Fig. 5(b) look very similar to results of massive two-dimensional QCD [22]. Other DLCQ calculations of two-dimensional massive QCD [23,24] were performed at finite N_c. In particular, it was shown in Ref. [23] that the spectrum of massive QCD in two dimensions is well described by the

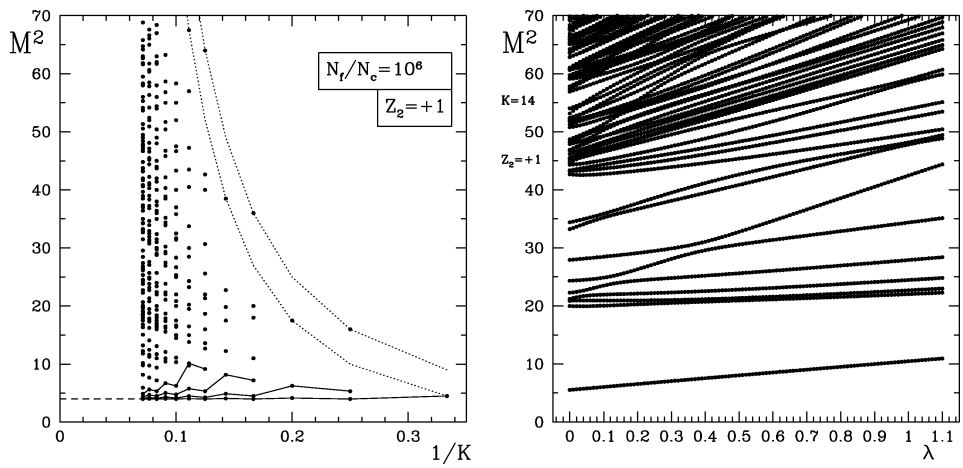

(a) (b)

Fig. 5. Left (a): Spectrum of the Z_2 even sector in large N_f limit. Note that masses are in units $g^2 N_f/\pi$. The dashed line is the extrapolation of the lowest eigenvalue towards the continuum. Right (b): Mass squared eigenvalues as functions of $\lambda = N_f/N_c$. Masses are in units $g^2 N_c/\pi$.

[7] M. Engelhardt [19] presented a truncated version of this calculation.

Table 2
Eigenvalues in the adjoint case, the 't Hooft limit and the large N_f limit. B_1 and B_2 are the lowest lying single particle states in the Z_2 even and odd sectors, respectively. The eigenvalue in the large N_f limit is actually the continuum threshold. Note that the masses are given in units $g^2 N_c/\pi$ in the first two cases and in units $g^2 N_f/\pi$ in the third

	$N_c = N_f$		$N_f/N_c \to 0$		$N_f/N_c \to \infty$
K	$M^2_{B_1}$	$M^2_{B_2}$	$M^2_{B_1}$	$M^2_{B_2}$	$M^2_{\text{cont.}}$
3	9.0000	18.0000	4.5000	9.0000	4.5000
4	9.4910	20.0000	4.7924	10.0000	4.0000
5	9.7815	21.2117	4.9835	10.6803	4.1666
6	9.9710	22.0078	5.1179	11.1724	4.0000
7	10.1034	22.5680	5.2176	11.5432	4.0888
8	10.2004	22.9811	5.2944	11.8326	4.0000
9	10.2742	23.2966	5.3553	12.0646	4.0500
10	10.3321	23.5446	5.4048	12.2545	4.0000
11	10.3784	23.7440	5.4458	12.4129	4.0333
12	10.4163	23.9074	5.4804	12.5469	4.0000
13	10.4478	24.0435	5.5099	12.6617	4.0238
14	10.4743	24.1583	5.5353	12.7612	4.0000
∞	10.84	25.73	5.88	14.11	4.00

large N_c approximation. Deviations from the large N_c behavior, found typically at small fermion masses m where the relevant coupling $g^2 N_c/m^2$ is strong, might just be artifacts of the DLCQ approach. This is in line with results of Ref. [13], showing that also in adjoint QCD in two dimensions the $1/N_c$ corrections are very small; a fact that still awaits proper explanation.

We see a lot of level crossings in Fig. 5(b). The fact that the trajectories do not intersect is a finite K effect. We note that the plot shows a smooth behavior at $\lambda = 1$. There is no hint that the adjoint case could be a special point in the parameter space. The eigenfunctions in the large N_f limit look very different than those found in the adjoint and the 't Hooft case. Typically, the amplitude vanishes, except for a few delta-like peaks, reflecting the fact that the spectrum of this theory consists of continuum states of non-interacting mesons. For comparison with other work, we list the eigenvalues obtained in the numerical calculations in the 't Hooft limit, with adjoint fermions and in the large N_f limit in Table 2.

5. Summary and discussion

In this note we studied two-dimensional QCD using $SU(N_c)$ currents as basic degrees of freedom. This enabled us to calculate the Hamiltonian matrix and the spectrum of any two-dimensional $SU(N_c)$ gauge theory coupled to an arbitrary number of fermions. Working in the DLCQ framework, all relevant quantities become functions of the parameter

$\lambda = N_f/N_c$ and of the harmonic resolution K. We constructed the Hamiltonian matrix explicitly in the Fock basis of single-trace states.

We reproduced all known results in the λ parameter space: in the 't Hooft limit ($\lambda \to 0$) we obtained the well-known linear spectrum, in the adjoint case we find exactly the eigenvalues of previous works [2,12,14], and we identified the single meson of the large N_f limit. Moreover, in the case of adjoint fermions we were able to confirm the single-particle nature of the lowest Z_2 odd boson, which was hidden in Ref. [12] among (trivial) multi-particle states which are absent in our calculation. We provided evidence for the single-particle nature of the boson B_3 at $M^2 = 45.99$, which makes the existence of other single-particle states above the continuum threshold at $M^2 = 4M_{F_1}^2$ very likely. We were able to explain the deformations in the trajectories of the eigenvalues as repulsions of eigenvalues. Unfortunately, the amount of remaining 'multi-particle' states in the spectrum makes it impossible to decide whether or not the identified single-particle states form an infinite Regge trajectory, or if even a multi-Regge structure exists, as was suggested in Ref. [21]. What we were able to do is to eliminate all states from the list of single-particle candidates which do not appear in our calculations, but in the bosonic sectors of previous works. By construction, our approach contains *all* single-particle states [6].

In Ref. [12] it was suggested the massless limit is reached only in the continuum limit $K \to \infty$. We work in a manifestly massless approach and obtain exactly the same eigenvalues for all K. It would be very interesting to repeat the calculation of Ref. [12] for finite m, as was done with different motivation in Ref. [14]. With our results at hand, one can focus on a much smaller set of single-particle candidates, and see how these states develop as the mass is turned on. Our guess is that this transition is continuous. An interesting related question is how to distinguish screening from confinement when only the mass spectrum is known.

We operate at higher numerical precision than previous work. This allowed us to prove numerically that the continuum threshold found in Ref. [12] is indeed exactly at four times the mass squared of the lightest fermion. We note however that the interpretation of the continuum states is not completely clear. We find that the deviation of their masses from the expected free many-body masses, Eq. (30), vanishes faster than $1/K^2$ as we go towards the continuum. If these states form a continuum at exactly the expected threshold, one has to conclude that they decouple completely from the single-particle states and that their coupling is an artifact of the finite resolution K.

To summarize, we presented a refined and quite coherent picture of two-dimensional QCD by using a new computational tool. We hope that this approach will prove powerful and that it will yield new qualitative insight, too. We mainly focused on quantitative improvements in the present work. We hope that this work will provide sufficient input for future enterprises to understand this theory, which shares some of the key features of full QCD, much better.

Acknowledgements

The author thanks D. Kutasov for initiating this work, involvement in the analytic calculations and for many discussions, and is grateful for the hospitality during visits at the University of Chicago. The author is grateful for many interesting discussions with A. Armoni, Y. Frishman and J. Sonnenschein and also acknowledges discussions with F. Antonuccio and S. Pinsky. A large part of this work was done while the author was supported by a Minerva Fellowship at the Weizmann Institute of Science, Rehovot, Israel. The hospitality at the Weizmann Institute is gratefully acknowledged. This work was supported in part by a Ohio State University Postdoctoral Fellowship.

References

[1] G. 't Hooft, Nucl. Phys. B 75 (1974) 461.
[2] S. Dalley, I.R. Klebanov, Phys. Rev. D 47 (1993) 2517.
[3] D. Kutasov, Nucl. Phys. B 414 (1994) 33.
[4] G.D. Date, Y. Frishman, J. Sonnenschein, Nucl. Phys. B 283 (1987) 365.
[5] A. Armoni, J. Sonnenschein, Nucl. Phys. B 457 (1995) 81.
[6] D. Kutasov, A. Schwimmer, Nucl. Phys. B 442 (1995) 447.
[7] A. Armoni, Y. Frishman, J. Sonnenschein, U. Trittmann, Nucl. Phys. B 537 (1998) 503.
[8] D.J. Gross, I.R. Klebanov, A.V. Matytsin, A.V. Smilga, Nucl. Phys. B 461 (1996) 109.
[9] Y. Frishman, J. Sonnenschein, Nucl. Phys. B 461 (1997) 285.
[10] A. Armoni, J. Sonnenschein, Nucl. Phys. B 502 (1997) 516.
[11] A. Armoni, Y. Frishman, J. Sonnenschein, Phys. Rev. Lett. 80 (1998) 430.
[12] D.J. Gross, A. Hashimoto, I.R. Klebanov, Phys. Rev. D 57 (1998) 6420.
[13] F. Antonuccio, S.S. Pinsky, Phys. Lett. B 439 (1998) 142.
[14] G. Bhanot, K. Demeterfi, I.R. Klebanov, Phys. Rev. D 48 (1993) 4980.
[15] A. Bassetto, hep-th/9809084.
[16] H.-C. Pauli, S.J. Brodsky, Phys. Rev. D 32 (1985) 1993.
[17] H.-C. Pauli, S.J. Brodsky, Phys. Rev. D 32 (1985) 2001.
[18] E. Witten, Commun. Math. Phys. 92 (1984) 455.
[19] M. Engelhardt, Nucl. Phys. B 440 (1995) 543.
[20] A. Armoni, private communication.
[21] J. Boorstein, D. Kutasov, in: J. Zinn-Justin (Ed.), Les Houches 1997, Elsevier, Amsterdam, 1997.
[22] A.J. Hanson, R.D. Peccei, M.K. Prasad, Nucl. Phys. B 121 (1977) 477.
[23] K. Hornbostel, S.J. Brodsky, H.-C. Pauli, Phys. Rev. D 41 (1990) 3814.
[24] M. Heyssler, A.C. Kalloniatis, Phys. Lett. B 354 (1995) 453.